World Journal of Advanced Research and Reviews
eISSN: 2581-9615 CODEN (USA): WJARAI
Cross Ref DOI: 10.30574/wjarr
Journal homepage: https://wjarr.com/

(CASE REPORT)

# CONCENTRIC RINGS WITHIN A RESTRICTED MASS: A CASE OF COEXISTING CHOLESTEATOMA AND MYCETOMA OF THE TEMPORAL BONE

Salma Abouchiba [1,*], Hanae Benazzouz [1], Wiame Bougrine [1], H. Ouazzani [2], Ismail Chaouche [1], Amal Akammar [2], Meriem Haloua [2], Badr Alami [1], Moulay Youssef Alaoui Lamrani [1], Meryem Boubbou P [2], Mustapha Maaroufi [1] and Nizar El Bouardi [1]

[1] Radiology Department, Hassan II University Hospital, University of Sidi Mohammed Ben Abdallah, Fez, Morocco.
[2] Mother and Child Radiology Department, Hassan II University Hospital, University of Sidi Mohammed Ben Abdallah, Fez, Morocco.
* Corresponding Author

ORCID Details
Salma Abouchiba : https://orcid.org/0009-0004-3571-9071

World Journal of Advanced Research and Reviews, 2026, 31(03), 440–446

Publication history: Received on 31 July 2026; revised on 07 September 2026; accepted on 09 September 2026

Article DOI: https://doi.org/10.30574/wjarr.2026.31.3.2324



## ABSTRACT

**Introduction:** Middle ear cholesteatoma is a well-recognized destructive lesion of the temporal bone. Colonization by a mycetoma arising within a cholesteatoma-generated bony cavity is an exceptionally rare and previously unreported complication. We report the first such case, compounded by three simultaneous complications: ossifying labyrinthitis, lateral semicircular canal fistula, and lateral sinus thrombosis extending to the internal jugular vein.

**Case Presentation:** A 42-year-old immunocompetent woman with a lifelong history of recurrent otitis media presented with a 3-month left fistulized otomastoiditis. HRCT and multiparametric MRI revealed a voluminous expansile mass centered on the left middle ear causing extensive petromastoid bone destruction. Within the cholesteatoma-generated cavity, a central fungal ball was identified by its characteristic laminated T2 signal pattern and absence of diffusion restriction on diffusion-weighted imaging — contrasting with the peripheral diffusion-restricting cholesteatoma matrix.

The coexistence of a macroscopic mycetoma within a cholesteatoma-sculpted mastoid cavity has not been previously described. Multiparametric MRI was essential in characterizing this dual pathology, providing non-redundant information to HRCT by resolving the two superimposed lesions, confirming lateral sinus thrombosis, and excluding intracranial extension. This case introduces the concept of cholesteatoma as a biological scaffold for mycetoma formation.

**Conclusion:** This case illustrates a unique and life-threatening constellation of complications arising from a neglected destructive cholesteatoma. Awareness of this dual pathology and systematic multiparametric imaging evaluation are essential for accurate diagnosis and surgical planning.

**Keywords:** Cholesteatoma; Mycetoma; Fungal ball; Mastoiditis; Lateral sinus thrombosis; Ossifying labyrinthitis; Temporal bone; MRI; DWI

## 1 INTRODUCTION

Acquired middle ear cholesteatoma is a well-recognized destructive lesion of the temporal bone, defined by the aberrant accumulation of a keratinizing squamous epithelial matrix within the middle ear and mastoid cavities. Through the sustained enzymatic activity of its epithelial lining, cholesteatoma induces progressive osteolysis, leading to ossicular chain destruction, labyrinthine fistula, intracranial extension, and vascular complications [1]. Despite the recognized prevalence of fungal organisms within cholesteatoma keratin debris on microbiological assay [2,3], the formation of a macroscopic, radiologically visible mycetoma within a cholesteatoma-generated bony cavity has never been described.

We report an exceptional case of a neglected left middle ear cholesteatoma in an immunocompetent adult, in which the bone-destructive activity of the lesion created a contained mastoid cavity subsequently colonized by an Aspergillus fumigatus mycetoma — a pathological constellation without precedent in the literature. This dual pathology was further compounded by three simultaneous severe complications: lateral semicircular canal fistula with ossifying labyrinthitis, and lateral sinus thrombosis extending to the internal jugular vein. We describe the clinical presentation, the multiparametric imaging findings that enabled characterization of both lesions, the surgical management, and histopathological confirmation, and discuss the pathophysiological mechanism underlying this unique complication.

## 2 CASE PRESENTATION

A 42-year-old immunocompetent woman was referred with a 3-month history of abundant left-sided purulent otorrhea and progressive retroauricular swelling. Her history was notable for recurrent otitis media since childhood, managed with repeated antibiotic courses without definitive surgical treatment. She denied prior ear surgery, trauma, or immunodeficiency, and had no comorbidities.

On admission, she was afebrile and hemodynamically stable, with no meningeal signs. Cranial nerve examination revealed a left peripheral facial nerve palsy (House-Brackmann Grade II) and mild intermittent vertigo without spontaneous nystagmus. Otoscopic examination showed a markedly stenosed left external auditory canal (EAC) filled with mucopurulent, foul-smelling otorrhea. A fistulous communication was identified between the mastoid region and the EAC through the posterior canal wall, and the tympanic membrane was not visualizable. The right ear was entirely normal. Audiological assessment revealed profound sensorineural hearing loss on the left, consistent with labyrinthine involvement.

Initial bloodwork showed a WBC of 12,500/mm$^3$ and CRP of 45 mg/L, likely attenuated by 6 days of pre-admission amoxicillin-clavulanate. Renal and hepatic function, blood glucose, and HIV serology were normal. Mycological cultures identified a polymicrobial flora alongside *Aspergillus fumigatus*, raising the possibility of a concomitant fungal co-infection in an immunocompetent host. Preoperatively, local care included a Pope otowick changed every 48 hours. Systemic antibiotic therapy comprising a third-generation cephalosporin, metronidazole, and vancomycin was initiated for 16 days pending definitive surgery.

### 2.1 Imaging Findings

#### 2.1.1 High-Resolution Computed Tomography (HRCT) of the Temporal Bone (Figure 1)

HRCT of the temporal bone demonstrated a voluminous expansile left middle ear lesion, isodense to soft tissue on unenhanced images with no contrast enhancement. The lesion contained coarse calcifications, hypodense zones, and interspersed air bubbles, with a fistulous tract communicating through the posterior EAC wall to the external skin surface. Extensive lytic destruction involved the mastoid tegmen, all middle ear cavity walls, and the lateral semicircular canal, producing a labyrinthine fistula. Marked hyperdensity of the vestibule and semicircular canals was consistent with ossifying labyrinthitis. A left lateral sinus thrombosis extending from the sigmoid sinus to the cervical internal jugular vein was identified as a major intracranial vascular complication **(Figure 2).**

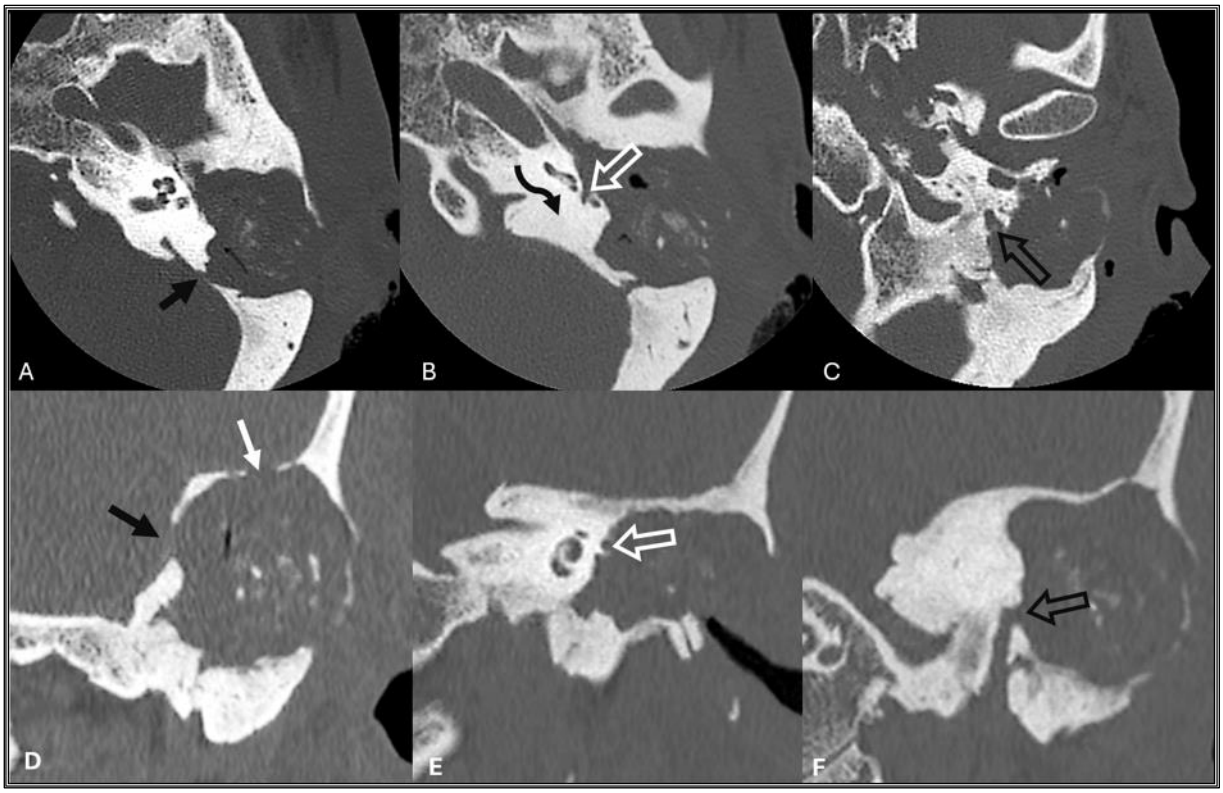


Extensive, lytic, and destructive mass originating from the left middle ear, causing widespread petromastoid bone destruction. The lesion is responsible for complete opacification and destruction of the mastoid antrum and air cells, associated with erosion of the tegmen antri **(white arrow)** and the cranial aspect of the mastoid cortex (black arrow). Additional findings include focal lytic destruction of the lateral wall of the lateral semicircular canal **(hollow white arrow),** resulting in a labyrinthine fistula with subsequent loss of the normal aerated appearance of the semicircular canals, which are nearly indistinguishable from bone density **(curved black arrow).** Finally, erosion of the stylomastoid canal wall is identified, providing the anatomical substrate for the peripheral facial nerve palsy documented clinically **(hollow black arrow).**

**Figure 1: Axial (A, B, C) and coronal (D, E, F) HRCT images of the left temporal bone**

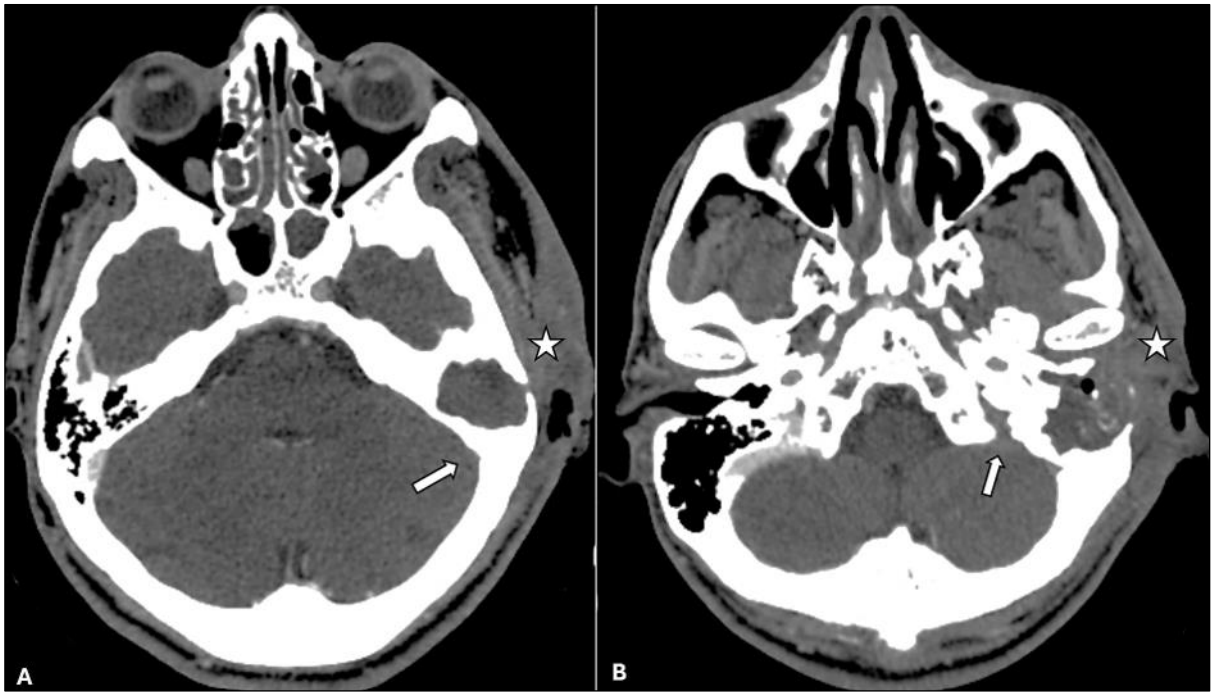


Pre- and retroauricular rim-enhancing collection containing internal air foci **(white star),** consistent with a small parts abscess in the setting of petromastoid destruction. Note the absence of opacification of the left lateral sinus **(white arrows),** indicative of lateral sinus thrombosis.

**Figure 2: Axial contrast-enhanced computed tomography of the brain (A, B)**

### 2.2 Multiparametric MRI of the Temporal Bone

MRI confirmed and further characterized the full extent of the lesion. The overall process appeared as a large expansile mass originating from the left middle ear, responsible for extensive petromastoid destruction with both breach of the external cortex and of the internal cortical plate, without definite intracranial extension.

The lesion demonstrated a distinctive dual-component signal architecture on multiparametric sequences:

Peripheral cholesteatoma component: The peripheral portion of the mass exhibited moderate T2 hyperintensity and, critically, marked diffusion restriction on DWI-HASTE sequences, the hallmark MRI signature of cholesteatoma keratin matrix. This component showed no contrast enhancement after gadolinium administration, consistent with a non-vascular avascular keratinous mass.

Central mycetoma component: The central portion of the lesion displayed a distinctive laminated signal pattern characteristic of a fungal ball: alternating concentric layers of T2 hypointensity, mild T2 hyperintensity, and complete T2 signal void (corresponding to calcified fungal elements and mineralized debris identified on CT). This central component showed no diffusion restriction and no contrast enhancement, distinguishing it unequivocally from granulation tissue.

The lateral sinus thrombosis was confirmed on MRI as loss of the normal flow void within the left sigmoid sinus and internal jugular vein, with signal characteristics suggesting a chronic thrombotic process. No definite intracranial extension of the infectious process, no meningeal enhancement, and no cerebral abscess were identified.

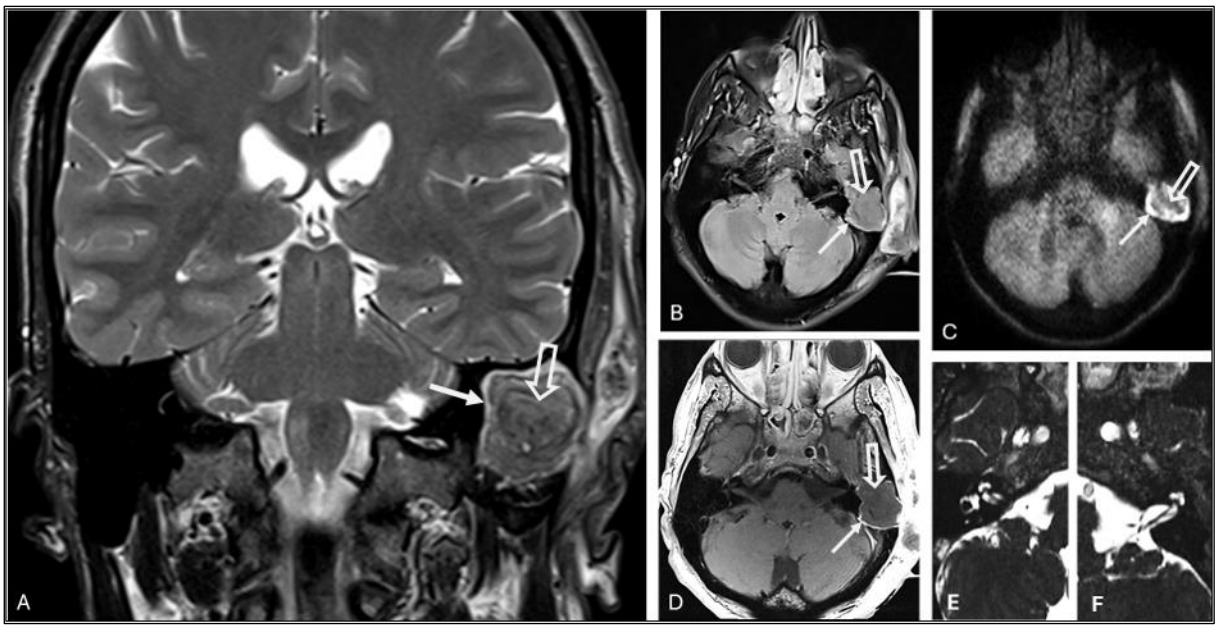


Coronal T2-weighted image **(A)** and axial T2 FLAIR **(B)** demonstrate a lesion with a dual-component architecture: a peripheral component showing mild T2 hyperintensity **(white arrow),** and a central component exhibiting a laminated pattern of alternating hypointense and signal-void layers, reminiscent of the concentric ring appearance characteristic of sinonasal fungal balls **(Hollow arrow).** Non-EPI HASTE diffusion-weighted imaging **(C)** reveals marked diffusion restriction confined to the peripheral component, consistent with cholesteatoma, while the central component shows no restricted diffusion, arguing against epithelial debris and supporting fungal etiology. Post-gadolinium T1-weighted imaging **(D)** demonstrates enhancement of the peripheral component with no enhancement of the central fungal mass. Additionally, the 3D SPACE sequence shows complete loss of fluid signal within the membranous labyrinth, involving the vestibule and semicircular canals, consistent with ossifying labyrinthitis.

**Figure 3: Multiparametric MRI of the temporal bone mass.**

The patient underwent left petromastoid exenteration via a retroauricular approach. Intraoperative findings confirmed extensive posterior EAC wall destruction, complete mastoid opacification by cholesteatoma matrix, and total ossicular chain erosion. A mycetoma was retrieved from the mastoid cavity and complete cholesteatoma excision was achieved. Enlargement meatoplasty was performed to ensure wide exteriorization for ventilation and surveillance.

Histopathology confirmed cholesteatoma with a keratin debris matrix lined by keratinizing squamous epithelium and a surrounding chronic inflammatory infiltrate with granulomatous features, consistent with advanced chronically active cholesteatoma.

Postoperatively, the patient received intravenous ceftriaxone, metronidazole, and corticosteroids, alongside antifungal therapy with voriconazole and therapeutic anticoagulation with low molecular weight heparin for the lateral sinus thrombosis.

## 3 DISCUSSION

This case represents, to our knowledge, the first documented instance of a middle ear cholesteatoma generating — through its own bone-destructive activity — a hollow mastoid cavity subsequently colonized by a macroscopic mycetoma, further compounded by three simultaneous severe complications: lateral semicircular canal fistula, ossifying labyrinthitis, and lateral sinus thrombosis extending to the internal jugular vein. Complete characterization was achievable only through combined HRCT and multiparametric MRI, each modality contributing indispensable and non-redundant diagnostic information.

HRCT remains the gold standard for mapping bony destruction in temporal bone disease, defining ossicular erosion, otic capsule involvement, tegmen dehiscence, and sinodural plate erosion with unmatched spatial resolution [1,2], but its inability to differentiate soft tissue pathologies — cholesteatoma, granulation tissue, effusion, and fungal material — renders it insufficient as a standalone modality in complex cases [3]. MRI was essential to resolve the nature of the two superimposed lesions, confirm sinus thrombosis, and exclude intracranial extension.

The peripheral component displayed marked diffusion restriction on non-EPI DWI-HASTE — the hallmark MRI signature of cholesteatoma, reflecting its dense water-impermeable keratin matrix [4]. Non-EPI sequences are now preferred over conventional EPI for temporal bone evaluation, as EPI is severely degraded by susceptibility artifacts at air–bone interfaces. A meta-analysis of 342 patients has established non-EPI DWI sensitivity and specificity for

cholesteatoma at 91–94% [5,6], with HASTE specifically outperforming RESOLVE in both primary and recurrent disease [7]. The circumferential distribution of diffusion restriction around a morphologically distinct central component was the key imaging observation prompting recognition of the dual-pathology architecture.

The central component presented an equally specific MRI signature: a laminated T2 architecture of alternating hypointense, mildly hyperintense, and signal-void layers, reflecting densely packed hyphae, proteinaceous debris, and paramagnetic heavy metal deposition producing progressive T2 suppression [8,9]. This pattern, well documented in sinonasal fungus balls where T2 hypointensity carries sensitivity approaching 100% [9,10], has never previously been described within the temporal bone. On CT, the central hyperdensity, coarse calcifications, and interspersed air bubbles closely replicate the established CT appearance of sinonasal mycetoma [8]. Crucially, the central component showed no diffusion restriction and no contrast enhancement — the precise inverse of the surrounding cholesteatoma — providing a clean multiparametric distinction between the two coexisting lesions, entirely invisible to HRCT alone.

HRCT demonstrated focal bony discontinuity of the lateral semicircular canal dome — the most common labyrinthine complication of cholesteatoma, reported in 5–10% of surgical series [11] — directly determining the surgical approach and the risk of iatrogenic sensorineural hearing loss [12]. Left vestibular and semicircular canal hyperdensity on CT, with corresponding loss of T2 fluid signal on MRI, are consistent with advanced tympanogenic ossifying labyrinthitis — the end-stage consequence of direct labyrinthine invasion through the eroded otic capsule. MRI detects early fibrous changes before CT abnormality becomes visible, while HRCT confirms established ossification [13,14]. The late ossification stage observed here implies irreversible vestibulo-labyrinthine destruction, directly relevant to audiological and vestibular rehabilitation planning.

Prior literature on fungal–cholesteatoma interaction has been limited to microscopic or cultural detection of fungal organisms within keratin debris, with prevalence rates of 42–75% on sensitive assays [15,16]. No previous report has described a macroscopic, radiologically visible fungal ball arising within a cholesteatoma-excavated bony cavity. The sole published radiological analogue — a mycetoma within a post-surgical mastoidectomy cavity [17] — differs fundamentally in that the cavity was surgically created. In the present case, the cholesteatoma itself, through enzymatic bone resorption, sculpted a contained anatomical niche providing the warm, protein-rich, microaerobic conditions required for macroscopic fungal ball formation. This concept of cholesteatoma as a biological scaffold for mycetoma is, to our knowledge, without precedent and constitutes the central scientific contribution of this report.

## 4 CONCLUSION

This case demonstrates that in any advanced cholesteatoma presenting with a heterogeneous internal architecture — particularly a laminated, T2-dark, non-restricting central component on MRI alongside a peripheral DWI-hyperintense rim — the possibility of superimposed mycetoma must be actively considered and explicitly reported, regardless of immune status. It further confirms that a complete multiparametric MRI protocol, including non-EPI DWI, T2-weighted, contrast-enhanced T1, and MR venography sequences, is indispensable in complicated temporal bone disease, where the clinical severity may dramatically underestimate the radiological burden, as illustrated by this afebrile patient harboring four simultaneous life-threatening complications.

## STATEMENTS ON COMPLIANCE WITH ETHICAL STANDARDS

### *Disclosure of conflict of interest*

The authors declare that they have no known competing financial interests or personal relationships that could have appeared to influence the work reported in this paper.

### *Statement of informed consent*

This case report was conducted in accordance with the ethical standards of the institutional guidelines of CHU Hassan II, Fès, Morocco, and with the 1964 Declaration of Helsinki and its later amendments. Formal ethics committee approval was not required for this case report per institutional policy, as it involves retrospective reporting of routine clinical care. Written informed consent was obtained from the patient for publication of this case report and any accompanying images.

## REFERENCES

[1] Sollmann N, et al. Imaging of pathologies of the temporal bone and middle ear. Tomography. 2023;9(6):2190–2210.

[2] Juliano AF, Ginat DT, Moonis G. Imaging review of the temporal bone: Part I. Radiology. 2013;269(1):17–33.

[3] Hiremath SB, Chakraborty S. Imaging the middle ear. In: Head and Neck Radiology. Radiology Key; 2024.

[4] Muzaffar J, et al. Diffusion-weighted MRI for residual and recurrent cholesteatoma. Cochrane Database Syst Rev. 2022.

[5] Li PM, et al. Evaluating the utility of non-EPI DWI in preoperative evaluation of cholesteatoma. Laryngoscope. 2013;123:1208–1213.

[6] Jindal M, et al. Systematic review of DWI MRI in postoperative cholesteatoma assessment. Otol Neurotol. 2011;32(8):1243–1249.

[7] Benson JC, et al. Non-EPI versus multishot EPI DWI in cholesteatoma detection. Am J Neuroradiol. 2021.

[8] ScienceDirect Topics. Fungus Ball. In: Diagnostic Imaging. Elsevier; 2024.

[9] Yoon JH, et al. MR findings of fungus ball: significance of high signal intensity on T1-weighted images. J Korean Med Sci. 2020;35(1):e22.

[10] Ogawa T, et al. Sinus fungus ball in the Japanese population: clinical and imaging characteristics of 104 cases. Int J Otorhinolaryngol. 2013.

[11] Copeland BJ, Buchman CA. Management of labyrinthine fistulae in chronic ear surgery. Am J Otolaryngol. 2003;24(1):51–60.

[12] Shivayogimath KN, et al. Our experience with labyrinthine fistula: prospective hearing outcomes. Indian J Otolaryngol Head Neck Surg. 2024;76(5):4493–4498.

[13] Çelik T, et al. The conundrum of labyrinthitis ossificans: an etiology-based case comparison. Turk Arch Otorhinolaryngol. 2024;61(4):183–187.

[14] Larson C, et al. Labyrinthitis ossificans. Applied Radiology. 2020.

[15] Singh GB, et al. Mycology of chronic suppurative otitis media–cholesteatoma disease. Am J Otolaryngol. 2018;39(2):157–161.

[16] He X, et al. Bacterial and fungal infections promote bone erosion in acquired cholesteatoma revealed by mNGS. Front Cell Infect Microbiol. 2021.

[17] Schubert R. Mycetoma in a mastoidectomy cavity (possible). Radiopaedia. Case rID-17620. 2022.